Received: 18 July 2019 | Revised: 17 November 2019 | Accepted: 5 December 2019

DOI: 10.1111/jfpe.13352

ORIGINAL ARTICLE

Journal of Food Process Engineering WILEY

High-pressure processing of pea protein–starch mixed systems: Effect of starch on structure formation

Shaun Y.J. Sim | Carmen I. Moraru

Department of Food Science, Cornell University, Ithaca, New York

Correspondence
Carmen I. Moraru, Department of Food Science, Cornell University, Ithaca, NY 14853.
Email: cim24@cornell.edu

Funding information
National Institute of Food and Agriculture, Grant/Award Number: 2016-67017-24635

Abstract

This work explores the structural effects of high-pressure processing (HPP) on starch in mixed pea protein–starch systems of varying concentrations. Reconstituted pea protein concentrate containing 9, 12, and 15% (w/w) protein, without added starch or in combination with 4 or 8% (w/w) pea starch, respectively, were subjected to HPP at 600 MPa for 4 min, at 5°C. Structural changes were investigated using dynamic rheology, scanning electron microscopy, and differential scanning calorimetry (DSC). The addition of starch enabled the formation of weak gels, at protein concentrations below the minimum required for gelation. Above the minimum protein concentration for gelation, starch addition resulted in stronger gels. Starch acted mainly as a filler in the pressure-induced protein gel matrix, and starch granules remained intact after HPP. DSC analyses confirmed that starch remained ungelatinized after HPP, likely due to the limited availability of water in the mixed systems during HPP.

Practical Applications

The structure of pressure-induced protein gels can be enhanced by adding starch. Besides being a low-cost ingredient, starch remains ungelatinized after high-pressure treatment, and thus can act like a fiber. Therefore, pressure-treated protein–starch mixtures may lead to the development of low-glycemic index, high-protein products.

1 | INTRODUCTION

The food industry is experiencing a growing demand for pulse proteins, due to their perceived health benefits and lower environmental impact of pulse crops (Henchion, Hayes, Mullen, Fenelon, & Tiwari, 2017). To capitalize on this trend, innovative processing methods are being explored to create new food products with interesting structures and textures using pulse proteins. An example of a suitable processing method is high-pressure processing (HPP). HPP, a nonthermal processing method used primarily for microbial inactivation, is able to disrupt noncovalent interactions, leading to protein denaturation and subsequent structural changes (Balasubramaniam, Martínez-Monteagudo, & Gupta, 2015; Cadesky, Walkling-Ribeiro, Kriner, Karwe, & Moraru, 2017). Unique gel structures can be formed above a minimum protein concentration by pressure-induced gelation of the denatured proteins (Queirós, Saraiva, & da Silva, 2018). The structural modifications induced by HPP in pea protein concentrates were recently explored (Sim, Karwe, & Moraru, 2019). Gel formation occurred from 12% (w/w) protein concentration and a pressure treatment at 250 MPa, with gel strength increasing with both pressure level and protein concentration. This was due to a greater extent of protein denaturation, aggregation, and network formation with increasing pressure levels.

Besides protein, starch is also a major component found in pulses, and pea protein concentrates contain a small amount of starch as well. This is important because HPP can also induce structural modifications in starch (Pei-Ling, Xiao-Song, & Qun, 2010). It has been reported before that in pure starch systems starch granules can be gelatinized by pressure, leading to gel formation (Ahmed, Singh, Ramaswamy, Pandey, & Raghavan, 2014; Leite, de Jesus, Schmiele,

Tribst, & Cristianini, 2017). The extent of starch pressure-induced gelatinization is influenced by starch type, applied pressure, temperature, hold time, and water content (Yang, Chaib, Gu, & Hemar, 2017). This suggests that starch could be a significant contributor to structure formation in pressure-treated protein gels.

Many food products (e.g., bread, pasta, and surimi) are made from protein–starch mixtures. Understanding how processing affects these mixtures could expand the food structure design toolbox. For example, the textural properties of heat-induced composite protein–starch gels can be controlled by adjusting protein–starch ratios and temperature in thermally-treated protein–starch mixtures (Joshi, Aldred, Panozzo, Kasapis, & Adhikari, 2014; Li, Yeh, & Fan, 2007). To date, there is little published information on the effect of pressure on starch in mixed protein–starch systems, some of which focus on animal-based proteins (Barrios-Peralta, Pérez-Won, Tabilo-Munizaga, & Briones-Labarca, 2012; Oh, Anema, Pinder, & Wong, 2009), and some on legume flours (Ahmed, Varshney, & Ramaswamy, 2009; Angioloni & Collar, 2013). In the latter, an increase in solid character of the flour dispersions was found after HPP treatment. Sim et al. (2019) found some evidence that starch granules in pea protein concentrates of high protein and low starch concentration were not gelatinized after HPP treatment. Therefore, the objective of this work was to investigate the role of starch in the pressure-induced structural changes in pea protein–starch systems of varying protein and starch concentrations.

2 | MATERIALS AND METHODS

2.1 | Pea protein concentrate and pea starch

Similar to previous work (Sim et al., 2019), pea protein concentrate (PPC) obtained by air classification (Pea Protein 55, AGT Foods, Regina, SK, Canada) was used as a source of pea protein. Pea protein isolate was not used, as preliminary investigation using differential scanning calorimetry (DSC) found that the proteins were denatured. The composition of PPC powder was: 54.5% (dry weight) protein, 4.3% (dry weight) starch, 2.8% (dry weight) fat, 6.7% (dry weight) ash, and 7.2% moisture. Pea starch (PS) was provided by World Food Processing LLC. (Turtle Lake, WI) and contained 0.7% (dry weight) protein, 94.0% (dry weight) starch, 0.1% (dry weight) fat, 0.15% (dry weight) ash, and 10.7% moisture. All compositions were determined at Dairy One Laboratories (Ithaca, NY).

2.2 | Sample preparation

Three protein concentrations of 9, 12, and 15% (w/w) were chosen to represent different structuring behavior. The minimum pea protein concentration for pressure gelation as determined by previous work was 12%, while 15% was close to the solubility limit of the PPC powder (Sim et al., 2019). To each protein concentration, PS was added to give final starch concentrations of 4 or 8% (w/w). These starch concentrations are comparable to existing protein–starch composite products such as surimi (Hunt, Getty, & Park, 2009). In total, nine formulations (9P, 9P/4S, 9P/8S, 12P, 12P/4S, 12P/8S, 15P, 15P/4S, and 15P/8S) were prepared. As a note, starch sedimentation was observed for less viscous systems of protein concentration below 9% (w/w) (Figure S1). This was not seen in mixed systems containing above 9% protein. An 8% (w/w) starch-only system, 8S, was made for comparison purposes. In the manuscript, the different mixtures will be referred to as *x*P/*y*S with *x*% protein and *y*% starch. *x*P represents the PPC-only system with *x*% protein, which only contains a small amount of starch. The complete composition information for all formulations is shown in Table 1.

To prepare the solutions, PPC and/or PS powders were added to Milli-Q water with stirring at 1,200 rpm for 30 min at 25°C. The solutions were then cooled in an ice bath with continued stirring for

TABLE 1 The protein and starch percentages in all formulations arranged in decreasing protein-to-starch ratios

Formulation	% protein (w/w)	% starch (w/w)	Protein-to-starch ratio	% total solids (w/w)	% moisture (w/w)
PPC powder	50.6	4.0	12.6	92.8	7.2
15P	15.0	1.19	12.6	27.5	72.5
12P	12.0	0.95	12.6	22.0	78.0
9P	9.0	0.71	12.6	16.5	83.5
15P/4S	15.0	4.0	3.8	30.5	69.5
12P/4S	12.0	4.0	3.0	25.3	74.7
9P/4S	9.0	4.0	2.3	20.0	80.0
15P/8S	15.0	8.0	1.9	34.8	65.2
12P/8S	12.0	8.0	1.5	29.5	70.5
9P/8S	9.0	8.0	1.1	24.3	75.7
Pea flour[a]	26.1	47.7	0.6	92.1	7.9
8S	<0.1	8.0	<0.01	8.5	91.5

[a]Average protein and starch percentages in pea flour according to Chung, Liu, Hoover, Warkentin, and Vandenberg (2008), shown for comparison purposes.

15 min. To achieve good dispersion, the solutions were subsequently high-shear mixed at 18,000 rpm for 7.5 min in an ice bath, using a high shear mixer (UltraTurrax Model T25 fitted with an S25N-18G dispersion tool, IKA Works, Inc., Wilmington, NC), ensuring that the solutions did not exceed 25°C. The pH of the PPC solutions was ~6.0. Finally, the mixed solutions were filled in pre-cut storage bags (FoodSaver Vacuum-Seal Roll, Sunbeam Products, Inc., Boca Raton, FL) and vacuum sealed. Each bag contained about 40 mL of sample. The packaged samples were stored overnight at 4°C before HPP treatment.

2.3 | HPP treatment

The samples were high-pressure processed using a 55 L HPP unit (Hiperbaric, Spain). Previously, it was found that gel formation occurred after 5 min at 550 MPa, with maximum gel strength occurring at 15 min hold time (Sim et al., 2019). However, the long hold times are not economically feasible for the food industry. Hence, in this study samples were subjected to a pressure of 600 MPa and a 4 min hold time, which are typical processing parameters used by the food industry for microbial inactivation (Buerman, Worobo, & Padilla-Zakour, 2020; Zhang et al., 2016). The initial temperature of the pressurizing medium (filtered water) was 5°C. The HPP unit was not equipped with sensors inside the vessel to track the temperature changes due to adiabatic heating, and the temperature of the water was monitored to assess any temperature changes. Since the samples occupied only a very small fraction of the HPP vessel (less than 1 L total volume for all samples out of the 55 L total volume of the vessel for each run), the temperature of the water was a good proxy for the temperature of the sample. Additionally, based on previously reported data, the adiabatic heating of water was found to lead to temperature increases of ~4°C/100 MPa (Grauwet, Van der Plancken, Vervoort, Hendrickx, & Van Loey, 2016). Therefore, for pressurization at 600 MPa of water with an initial temperature of 5°C, the maximum temperature reached would be ~30°C, which is much lower than the temperatures where starch gelatinization and protein denaturation occur. However, only minimal changes in the measured water temperatures were detected after the HPP runs, since the stainless steel vessel was also chilled. The HPP-treated samples were stored at 4°C to minimize microbial activity, and analyzed within 48 hr. Three independent sample preparations and subsequent treatments were conducted for each formulation.

2.4 | Rheological analyses

Dynamic rheological testing of the samples was conducted using an ARES strain-controlled rheometer (TA Instruments, New Castle, DE) as described previously (Sim et al., 2019). For samples of softer consistency, a 50 mm diameter Teflon parallel plate with an interplaten gap of 1 mm was used. Two mL aliquots of the protein sample were loaded onto the lower plate, with care taken to avoid air bubble formation. For stronger gel samples, a 25 mm diameter Teflon parallel plate with an interplaten gap of 2 mm was used. The gels were sliced 2 mm thick and placed between the plates.

All measurements were performed at 25°C, maintained using a Peltier temperature control system. An isothermal chamber enclosed the parallel plates to minimize sample dehydration during measurements. The samples were subjected to a 1 min relaxation step before measurements. Dynamic strain sweeps were first conducted for each sample to identify the linear viscoelastic region (LVR), at a frequency of 1 rad/s. Frequency sweeps were then performed at a strain value within the LVR, over the frequency range 0.1–100 rad/s. The storage modulus (G'), loss modulus (G''), and loss tangent ($\tan\delta = G''/G'$) were recorded. The storage modulus at 1 rad/s ($G'_{1\ \mathrm{rad/s}}$) and a frequency dependence parameter (m) were used to make direct comparisons between samples. m is the slope of the log(prevailing modulus) vs. log(frequency) curve. The prevailing modulus was chosen as G' for samples with solid-like behavior and G'' for liquid-like behavior. All measurements were performed in triplicate. No rheological measurements were conducted for 8% starch-only samples due to sedimentation of the untreated sample, and phase separation of the HPP-treated sample.

2.5 | Microstructural analyses by scanning electron microscopy (SEM)

Small amounts of untreated and HPP-treated 15P PPC-only and 15P/8S mixed samples, and the solid phase of HPP-treated 8S starch-only sample were deposited onto clean glass slides and air dried for 40 min. Thin cross-sections were used for strong gel samples. To minimize structural changes, a sample preparation method suitable for biological samples was used (Murtey & Ramasamy, 2016). Samples were fixated with 2.5% (w/v) glutaraldehyde in 0.05 M sodium cacodylate buffer for 2 hr, and washed three times for 5 min each with the cacodylate buffer. A secondary fixation was done using 1% (w/v) osmium tetroxide in cacodylate buffer for 1 hr, and samples washed three times in the cacodylate buffer. Samples were then dehydrated using graded ethanol solutions in the order 25, 50, 70, 95% (v/v) and three times with 100% (v/v) for 10 min each, followed by critical point drying using carbon dioxide. Dried surfaces were mounted on SEM stubs with carbon tape, then thinly coated with a gold/palladium alloy. A Zeiss LEO 1550 field emission scanning electron microscope (Carl Zeiss Microscopy LLC, Jena, Germany) was used for imaging at 3 kV. Images were acquired using the SmartSEM software accompanying the instrument.

2.6 | Differential scanning calorimetry

The DSC protocol was adapted from Ahmed et al. (2014). Thermograms of untreated and HPP-treated samples were obtained using a differential scanning calorimeter (DSC Model Q1000, TA

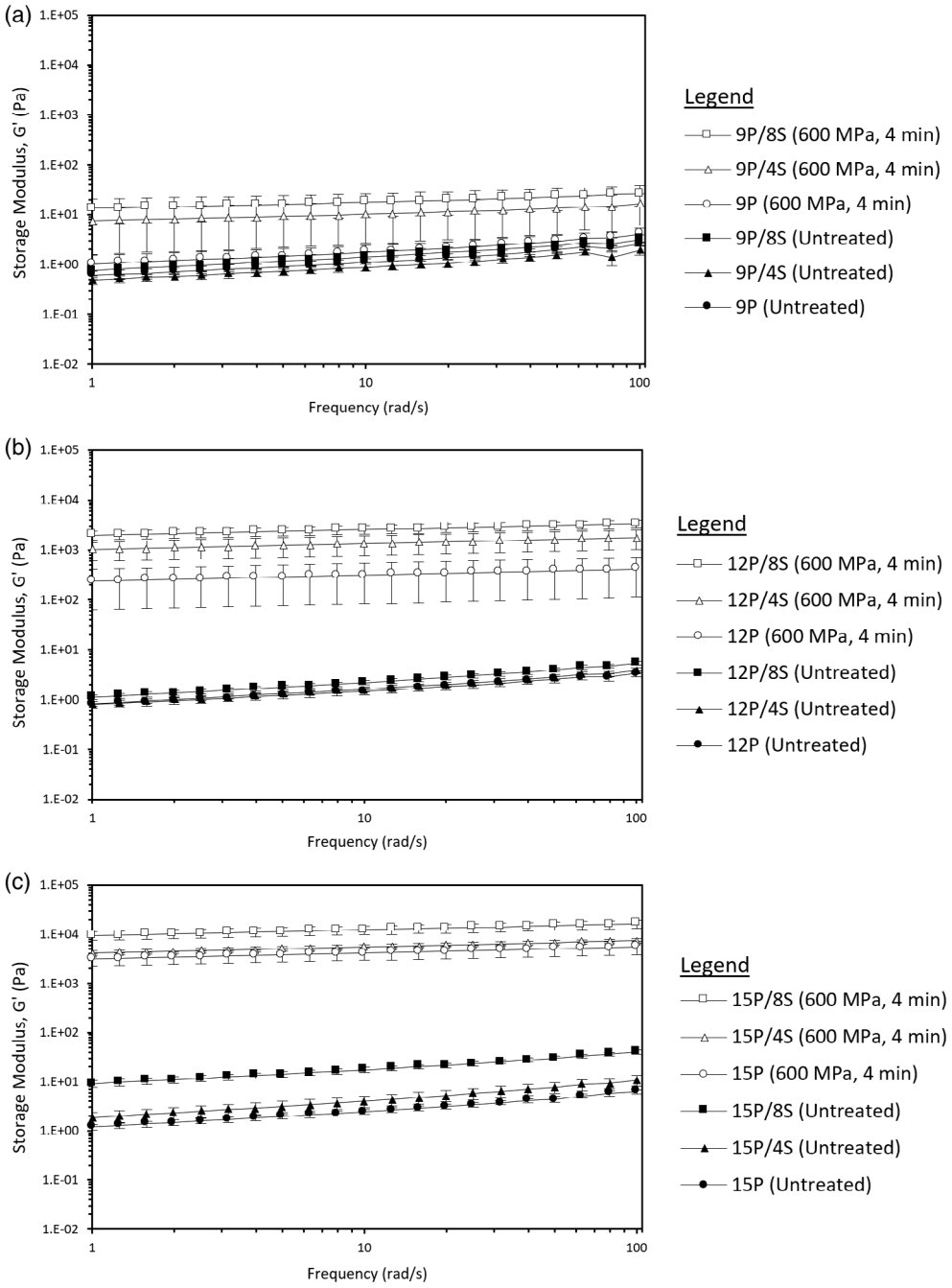

FIGURE 1 Frequency sweeps (G' vs. frequency) for untreated and pressure-treated PPC-only and mixed protein–starch samples, at different protein concentrations: (a) 9, (b) 12, and (c) 15% (w/w). Starch concentration in the mixed samples was 4% or 8% (w/w). Error bars represent 1 *SD* (n = 3)

Instruments, New Castle, DE), which was calibrated using indium and sapphire standards. A heat-treated (95°C for 15 min, followed by quenching in an ice bath for 15 min) 8S sample was also measured for comparison. The solid phases of the heat-treated and pressure-treated 8S samples were blended, respectively, with their liquid phases before measurement, to ensure comparable water content with the untreated sample. Samples (20–30 mg each) were weighed into DSC aluminum pans, which were then hermetically sealed and scanned between 15 and 110°C, at a heating rate of 2°C/min. An empty hermetically sealed aluminum pan was used as reference. The onset temperature (T_{onset}), peak temperature (T_{peak}), and the enthalpy (ΔH) of thermal transitions were calculated by manual peak integration using the equipment software (TA Instruments, New Castle, DE). Merged peaks were deconvoluted using Origin 9 software (OriginLab Corp., Northampton, MA) with Gaussian curve fitting function (adjusted R^2 values above .99). The enthalpy of deconvoluted peaks was calculated from the relative integral area of the fitted curve. All measurements were performed in triplicate.

2.7 | Statistical analysis

Statistical analysis was performed using R v. 3.2.2 (R Foundation for Statistical Computing, Vienna, Austria). A one-way analysis of variance (ANOVA) was conducted to determine if the mean values of

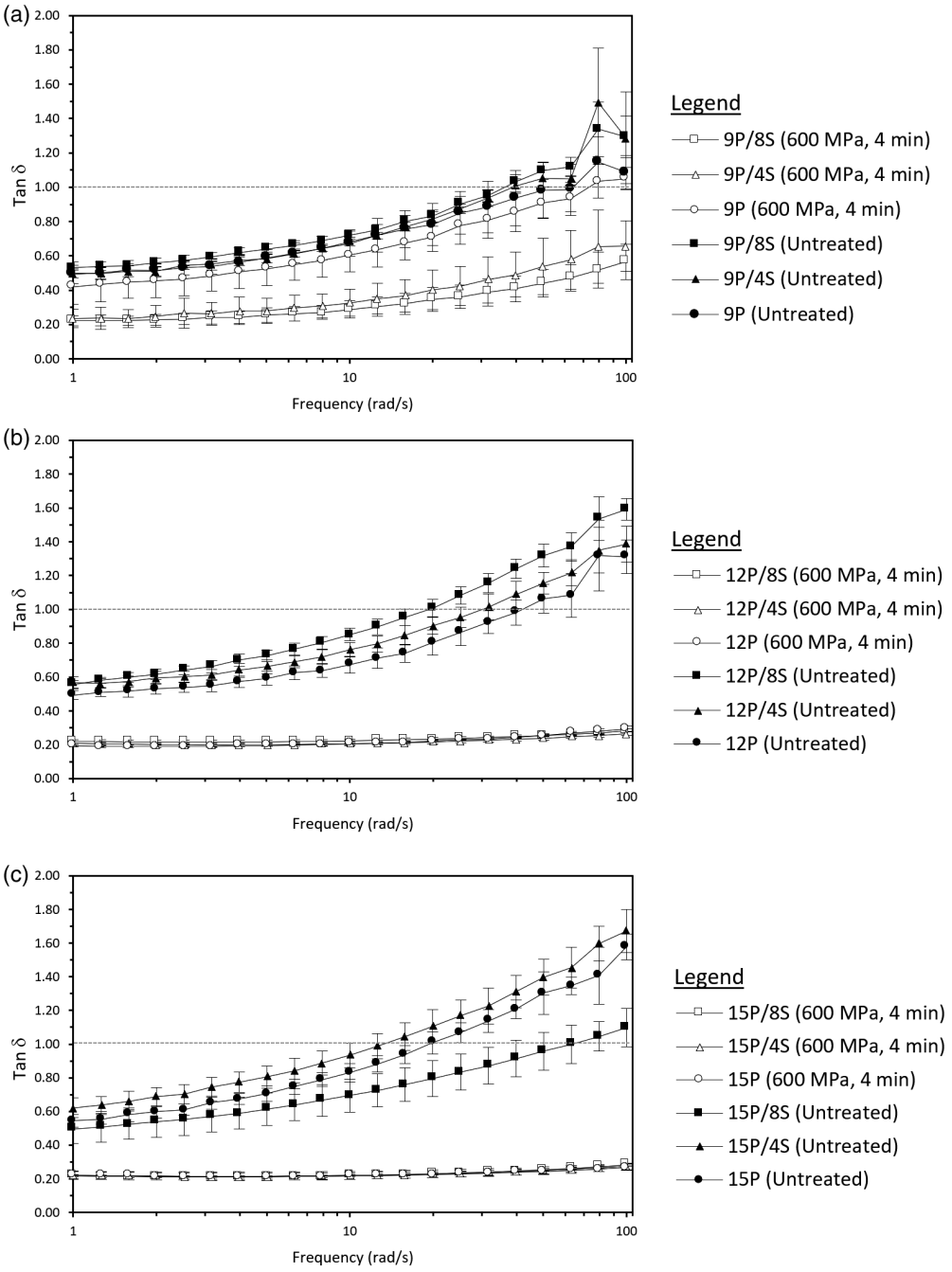

FIGURE 2 Tan δ vs. frequency for untreated and pressure-treated PPC-only and mixed protein–starch samples, at different protein concentrations: (a) 9, (b) 12, and (c) 15% (w/w). Starch concentration in the mixed samples is 4 or 8% (w/w). Error bars represent 1 *SD* (n = 3)

measured parameters differed significantly as a function of formulation and treatment. The significance was established using Tukey HSD post hoc tests. A probability level of $p < .05$ was considered significant. All values were expressed as means ±1 *SD*.

3 | RESULTS

3.1 | Effect of HPP on the rheological properties of the PPC-only and mixed systems

Figures 1 and 2 show frequency sweeps of untreated and pressure-treated samples. Tan $\delta < 1$ (hence $G' > G''$) for all samples, except untreated samples at frequencies above 10 rad/s. The rheological behavior of the different samples was evaluated by comparing G' values at 1 rad/s ($G'_{1\ rad/s}$) and the slope of the G' vs frequency curves (m), respectively.

For the untreated samples, while there were no significant differences among different formulations, $G'_{1\ rad/s}$ increased with total solids content (Figure 3). The untreated samples had tan δ values between 0.5 and 1.7, and frequency parameter m values between 0.31 and 0.38 (Figure 4). These values are indicative of a weakly associated concentrated dispersion (Beliciu & Moraru, 2013). Most untreated samples had a liquid-like behavior, even when starch was added (Figure 2). Interestingly, the tan δ values for the 15P/8S mixed samples were smaller than for the other samples, suggesting an

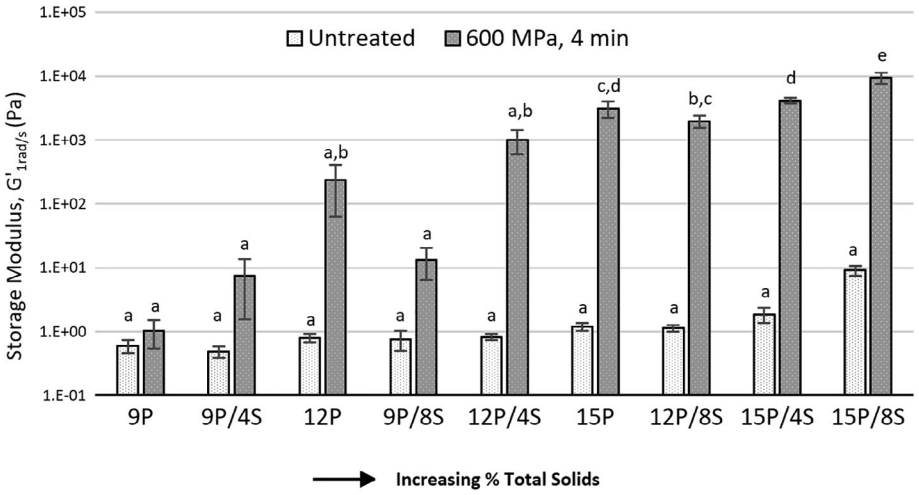

FIGURE 3 Storage modulus at 1 rad/s ($G'_{1\ rad/s}$) for untreated and pressure-treated PPC-only and mixed protein–starch samples with increasing total solids content. *x*P represents PPC-only systems with *x*% protein, and *x*P/*y*S represents mixed systems with *x*% protein and *y*% starch. Error bars represent 1 *SD* (n = 3). Data points connected by the same letter are not significantly different from each other (p > .05)

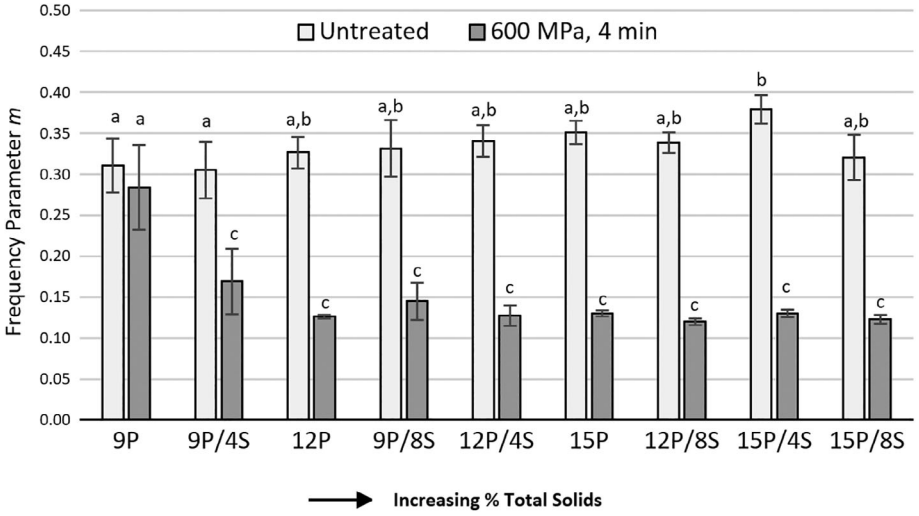

FIGURE 4 Frequency dependence parameter *m* of untreated and pressure-treated PPC-only and mixed protein–starch samples with increasing total solids content. *x*P represents PPC-only systems with *x*% protein, and *x*P/*y*S represents mixed systems with *x*% protein and *y*% starch. Error bars represent 1 *SD* (n = 3). Bars with the same letter are not significantly different from each other (p > .05)

increase in the solid-like character, possibly due to lower mobility of the components in the highly concentrated system.

$G'_{1\ rad/s}$ values increased by up to three orders of magnitude for HPP-treated samples compared to untreated samples (Figure 3). For each protein concentration, $G'_{1\ rad/s}$ increased with starch concentration. Gel formation did not occur for the pressure-treated 9P PPC-only samples, as evidenced by $\tan\delta$ between 0.4 and 1.0 and no significant decrease in *m* value after HPP treatment, since the protein concentration was below the minimum protein concentration for gelation (Sim et al., 2019). Weak gels were however formed with the addition of starch for the pressure-treated 9P/4S and 9P/8S mixed samples ($\tan\delta$ between 0.2–0.7 and *m* values of 0.15–0.17 after HPP treatment). HPP treatment of the 12 and 15% protein concentration PPC-only and mixed systems resulted in even smaller $\tan\delta$ (between 0.2 and 0.3) and *m* (~0.1), which are characteristic of strong gels (Steffe, 1996). In particular, self-standing gels were formed when starch was added to 12P samples ($G'_{1\ rad/s}$ ~ 10^3 Pa). Notably, gel strength was more dependent on protein concentration than the increase in total solids from added starch. For example, pressure-treated 12P samples had higher $G'_{1\ rad/s}$ than pressure-treated 9P/8S mixed samples, even though the latter had a greater total solids content. A similar behavior was also seen in pressure-treated 15P and 12P/8S samples.

3.2 | Microstructural observations of untreated and HPP-treated samples

Even though the samples were well mixed just prior to HPP treatment, HPP treated 8% starch-only (8S) samples showed macroscopic phase separation into a solid phase and a liquid phase, which is consistent with the findings reported by Leite et al. (2017) for pea starch solutions treated at pressures above 500 MPa. The solid phase was analyzed by SEM, and was found to consist of intact, disrupted, and fused starch granules (Figure 5). Sedimentation and subsequent pressure-driven compacting of the dense starch granules during the pressure ramp-up and hold time could have led to phase separation. The starch granules remained fused even after pressure was released.

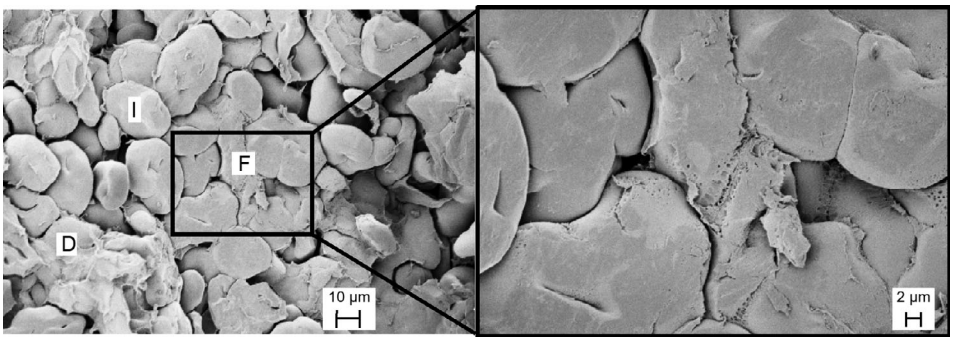

FIGURE 5 SEM micrographs of the solid phase of pressure-treated 8% (w/w) starch-only (8S) sample. The solid phase is composed of intact (I), disrupted (D), and fused (F) starch granules

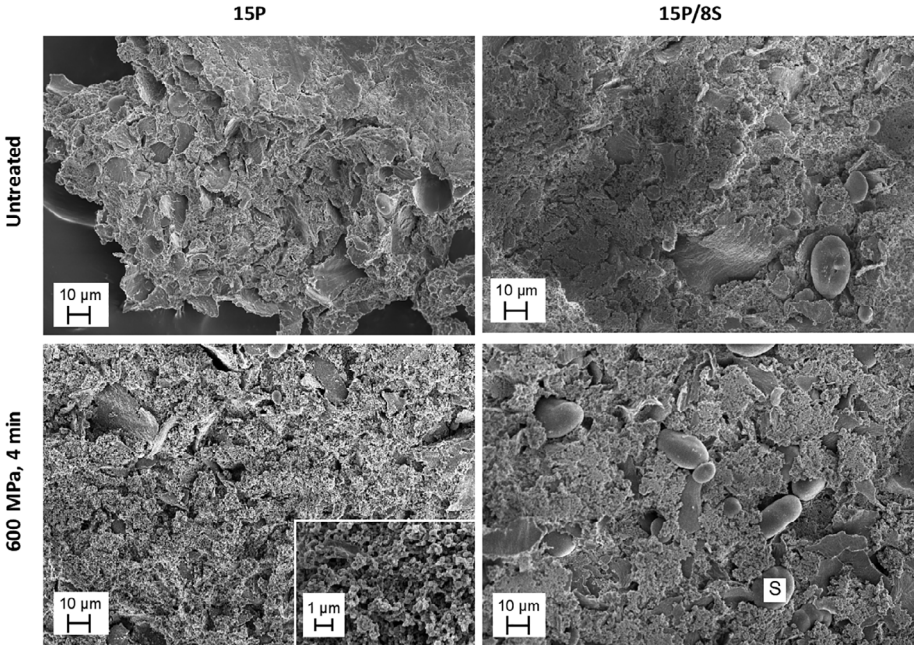

FIGURE 6 SEM micrographs of untreated and pressure-treated 15% (w/w) protein PPC-only (15P), and 15% (w/w) protein with 8% (w/w) starch mixed (15P/8S) samples. The PPC-only samples naturally contain a small amount of starch. The insert shows the protein gel formed by a network of aggregates. More starch granules (S) are seen embedded in the protein network for the 15P/8S samples

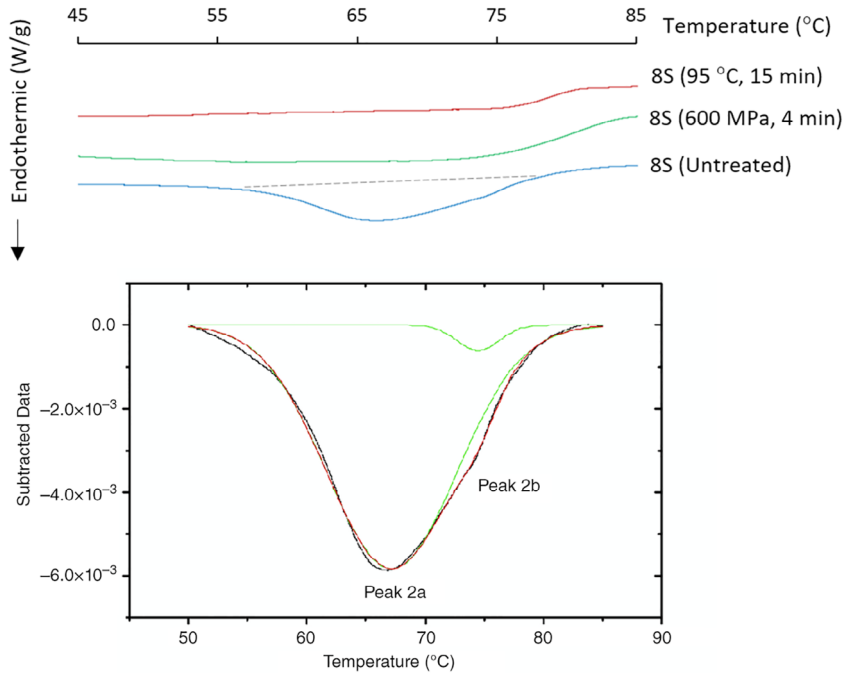

FIGURE 7 Top: DSC thermograms for untreated, pressure-treated, and heat-treated 8% (w/w) starch-only (8S) samples. Bottom: deconvolution of the untreated 8S sample gives Peaks 2a and 2b

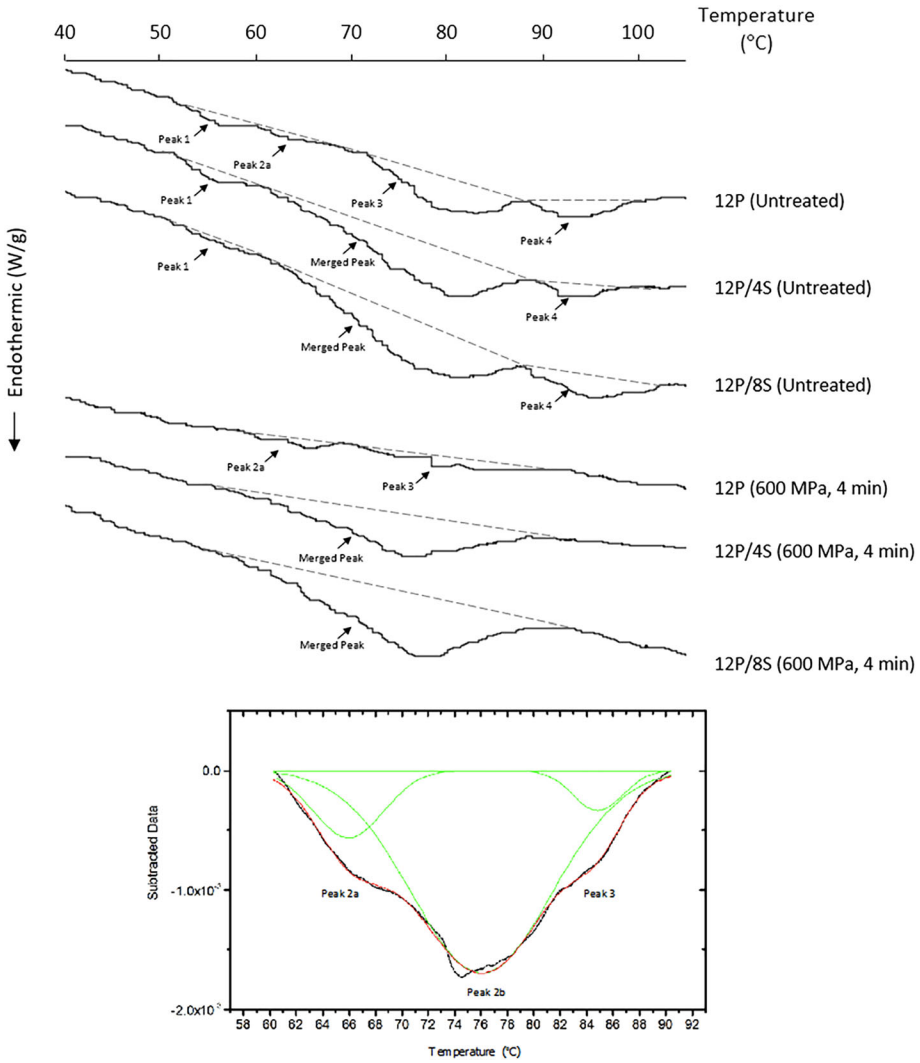

FIGURE 8 Top: DSC thermograms for untreated and pressure-treated 12% (w/w) protein PPC-only (12P), and 12% (w/w) protein with 4% or 8% (w/w) starch mixed (12P/4S or 12P/8S) samples. The thermogram is also representative for 9% and 15% (w/w) protein concentration samples. Bottom: deconvolution of the merged peak yields Peaks 2a, 2b, and 3

SEM imaging was also conducted on untreated and pressure-treated 15P and 15P/8S samples (Figure 6). As shown in the insert for the HPP-treated 15P sample, the gel structure was made up by a network of protein aggregates. More starch granules were seen in the 15P/8S samples than the 15P samples. The intact starch granules were embedded in the protein network and seemed to behave as a filler. Unlike the 8S samples, phase separation did not occur, likely due to reduced starch sedimentation in the more viscous PPC solutions, and the entrapment of the starch granules in the protein matrix when pressure was released.

3.3 | Effect of HPP on thermal transitions in the PPC-only and mixed systems

Thermal analyses by DSC were conducted for untreated, pressure-treated, and heat-treated 8S starch-only samples, and all PPC-only and mixed samples. The DSC thermograms are shown in Figures 7 and 8, the characteristic temperatures (onset and peak) and enthalpy of the identified thermal transitions are summarized in Table 2, and the identification of these peaks is discussed below.

For the 8S untreated starch-only sample, one peak (T_{peak} ~ 66°C) was observed (Figure 7), which corresponds to the gelatinization of pea starch (Ratnayake, Hoover, Shahidi, Perera, & Jane, 2001). Deconvolution of this peak revealed two peaks: Peak 2a (T_{peak} ~ 64°C) and Peak 2b (T_{peak} ~ 71°C), which corresponds to the B-type and A-type polymorphs of pea starch, respectively (Bogracheva, Morris, Ring, & Hedley, 1998).

For the untreated PPC-only samples, four major peaks were observed (Figure 8, top). Peak 1 (T_{peak} ~ 56°C) was attributed to the melting of endogenous lipid crystals (Eliasson, 1994); Peak 2a (T_{peak} ~ 65°C), as discussed above, corresponds to the gelatinization of B-type crystal form of starch; Peak 3 (T_{peak} ~ 81°C) corresponds to protein denaturation (Shand, Ya, Pietrasik, & Wanasundara, 2007); and Peak 4 (T_{peak} ~ 94°C) to the dissociation of amylose–lipid complexes formed during starch gelatinization, between leached amylose and the endogenous lipids (Eliasson, 1994).

For the untreated mixed samples, in addition to Peak 1 and Peak 4, a large peak with T_{peak} ~ 74°C was observed (Figure 8, top). This is

TABLE 2 Thermal transition parameters identified for untreated and pressure-treated mixed pea protein–starch solutions

	T_{onset} (°C)		T_{peak} (°C)		ΔH (J/g component)	
Sample	Untreated	600 MPa, 4 min	Untreated	600 MPa, 4 min	Untreated	600 MPa, 4 min
Peak 1 (lipid)						
9P	53.25 ± 0.39*a*	n.d.	56.22 ± 0.05*a*	n.d.	4.26 ± 1.15*ab*	n.d.
9P/4S	53.24 ± 0.42*a*	n.d.	55.35 ± 0.17*a*	n.d.	1.67 ± 0.06*a*	n.d.
9P/8S	53.70 ± 1.56*a*	n.d.	55.82 ± 0.58*a*	n.d.	2.45 ± 1.76*a*	n.d.
12P	52.05 ± 2.13*a*	n.d.	56.64 ± 0.90*a*	n.d.	6.55 ± 1.90*abc*	n.d.
12P/4S	53.24 ± 0.51*a*	n.d.	56.25 ± 0.97*a*	n.d.	4.83 ± 2.00*abc*	n.d.
12P/8S	52.91 ± 1.42*a*	n.d.	55.82 ± 0.84*a*	n.d.	3.23 ± 1.42*ab*	n.d.
15P	52.87 ± 1.82*a*	n.d.	56.20 ± 1.36*a*	n.d.	9.85 ± 2.44*c*	n.d.
15P/4S	52.19 ± 0.72*a*	51.39 ± 4.79*a*	56.18 ± 0.06*a*	54.49 ± 3.61*a*	8.66 ± 1.84*bc*	3.58 ± 2.77*ab*
15P/8S	52.40 ± 0.48*a*	n.d.	55.73 ± 0.23*a*	n.d.	4.21 ± 1.75*ab*	n.d.
8S	n.d.	n.d.	n.d.	n.d.	n.d.	n.d.
Peak 2a (starch)						
9P	61.81 ± 2.09*ab*	58.30 ± 0.55*a*	63.12 ± 1.63*a*	64.64 ± 0.86*abc*	1.53 ± 1.50*a*	6.24 ± 0.94*bc*
9P/4S			65.38 ± 0.62*abc*	68.25 ± 2.65*bc*	0.87 ± 0.14*a*	9.19 ± 4.42*c*
9P/8S			66.93 ± 1.11*abc*	66.24 ± 1.36*abc*	1.58 ± 1.45*ab*	3.08 ± 1.06*ab*
12P	61.88 ± 0.94*ab*	61.96 ± 0.54*ab*	64.91 ± 0.79*abc*	65.75 ± 0.60*abc*	2.05 ± 0.62*ab*	4.00 ± 1.17*ab*
12P/4S			66.62 ± 0.41*abc*	66.20 ± 0.60*abc*	1.92 ± 1.05*ab*	3.05 ± 1.54*ab*
12P/8S			68.38 ± 0.26*bc*	66.57 ± 0.66*abc*	1.91 ± 0.85*ab*	2.45 ± 0.34*ab*
15P	64.72 ± 2.12*b*	63.08 ± 1.23*b*	66.96 ± 1.51*abc*	66.65 ± 0.53*abc*	2.00 ± 1.16*ab*	5.77 ± 1.87*abc*
15P/4S			68.47 ± 1.05*bc*	67.01 ± 0.15*abc*	2.58 ± 0.73*ab*	2.63 ± 1.16*ab*
15P/8S			68.71 ± 0.96*c*	68.48 ± 0.53*c*	2.48 ± 1.06*ab*	4.02 ± 1.12*ab*
8S			64.41 ± 3.81*ab*	n.d.	31.84 ± 22.24	n.d.
Peak 2b (starch)						
9P	n.d.	n.d.	n.d.	n.d.	n.d.	n.d.
9P/4S			73.57 ± 0.21*ab*	74.93 ± 0.70*bc*	18.80 ± 4.46*a*	5.83 ± 4.95*a*
9P/8S			74.49 ± 0.73*abc*	74.77 ± 0.32*bc*	10.13 ± 2.73*a*	6.40 ± 2.97*a*
12P	n.d.	n.d.	n.d.	n.d.	n.d.	n.d.
12P/4S			75.44 ± 0.73*bcd*	76.12 ± 0.62*bcde*	16.64 ± 12.12*a*	13.93 ± 2.07*a*
12P/8S			76.56 ± 0.37*bcde*	76.85 ± 0.32*bcde*	10.84 ± 3.81*a*	12.56 ± 2.10*a*
15P	n.d.	n.d.	n.d.	n.d.	n.d.	n.d.
15P/4S			78.77 ± 0.11*de*	77.78 ± 0.74*cde*	13.04 ± 1.30*a*	12.15 ± 1.73*a*
15P/8S			77.91 ± 0.50*cde*	78.78 ± 0.35*e*	11.92 ± 0.59*a*	13.48 ± 1.01*a*
8S			71.01 ± 3.95*a*	n.d.	11.62 ± 10.57*a*	n.d.
Peak 3 (protein)						
9P	70.52 ± 1.00*a*	80.16 ± 2.06*c*	79.26 ± 0.83*a*	84.17 ± 0.38*cde*	2.49 ± 0.11*de*	0.39 ± 0.14*a*
9P/4S			82.20 ± 0.92*bcd*	82.71 ± 2.58*bcd*	0.76 ± 0.57*abc*	0.81 ± 0.82*abc*
9P/8S			82.50 ± 0.47*bcd*	83.06 ± 1.17*bcd*	0.89 ± 0.35*abc*	0.93 ± 0.82*abc*
12P	73.53 ± 1.08*ab*	77.88 ± 3.11*bc*	80.97 ± 1.78*ab*	84.30 ± 0.50*cde*	2.69 ± 0.19*de*	0.70 ± 0.49*abc*
12P/4S			82.62 ± 0.85*bcd*	84.86 ± 0.96*de*	1.71 ± 0.64*bcd*	0.58 ± 0.19*ab*
12P/8S			83.61 ± 0.34*bcde*	86.11 ± 0.17*e*	1.12 ± 0.40*abc*	0.35 ± 0.01*a*
15P	73.66 ± 0.13*ab*	73.24 ± 2.65*ab*	81.90 ± 0.58*abc*	84.05 ± 0.75*cde*	3.15 ± 0.28*e*	0.72 ± 0.16*abc*
15P/4S			84.00 ± 0.11*cde*	86.22 ± 0.29*e*	1.51 ± 0.29*abcd*	0.28 ± 0.15*a*
15P/8S			84.62 ± 0.25*cde*	86.27 ± 0.53*e*	1.93 ± 0.04*cde*	0.67 ± 0.39*ab*
8S	n.d.	n.d.	n.d.	n.d.	n.d.	n.d.

(Continues)

TABLE 2 (Continued)

Sample	T_{onset} (°C)		T_{peak} (°C)		ΔH (J/g component)	
	Untreated	600 MPa, 4 min	Untreated	600 MPa, 4 min	Untreated	600 MPa, 4 min
Peak 4 (amylose–lipid complex)						
9P	87.16 ± 0.32*a*	93.10 ± 0.88*cde*	92.14 ± 0.81*a*	95.33 ± 1.28*bcd*	18.91 ± 8.99*abc*	3.34 ± 1.33*a*
9P/4S	88.40 ± 0.37*ab*	94.86 ± 3.68*e*	92.44 ± 0.82*ab*	97.44 ± 2.07*d*	18.85 ± 6.61*abc*	7.76 ± 4.50*ab*
9P/8S	88.69 ± 0.27*ab*	n.d.	93.69 ± 1.29*abc*	n.d.	16.02 ± 1.85*abc*	n.d.
12P	89.50 ± 0.71*abc*	n.d.	93.78 ± 0.50*abc*	n.d.	18.02 ± 6.02*abc*	n.d.
12P/4S	89.87 ± 0.22*abcd*	n.d.	94.01 ± 0.80*abc*	n.d.	21.53 ± 3.61*bc*	n.d.
12P/8S	89.94 ± 1.51*abcd*	n.d.	94.93 ± 0.17*abcd*	n.d.	28.69 ± 7.72*c*	n.d.
15P	90.00 ± 0.47*abcd*	n.d.	94.68 ± 0.58*abcd*	n.d.	28.26 ± 2.06*c*	n.d.
15P/4S	91.40 ± 0.60*bcde*	93.64 ± 1.86*de*	95.78 ± 0.93 *cd*	97.34 ± 1.18*d*	30.82 ± 9.26*c*	2.25 ± 1.14*a*
15P/8S	92.28 ± 0.58*bcde*	n.d.	96.37 ± 0.48 *cd*	n.d.	26.55 ± 10.11*c*	n.d.
8S	n.d.	n.d.	n.d.	n.d.	n.d.	n.d.

Notes: *x*P represents PPC-only systems with *x*% protein, *x*P/*y*S represents mixed systems with *x*% protein and *y*% starch, and 8S represents the starch-only system with 8% starch. The enthalpy of Peak 4 was calculated per gram of lipid. For each peak, untreated and pressure-treated values of each parameter (T_{onset}, T_{peak}, and ΔH) connected by the same letter are not significantly different from each other ($p > .05$). No T_{onset} values for deconvoluted samples were available and therefore left blank. n.d.: not detected. Values represent averages of three replicates ±1SD.

consistent with the findings of Chung, Liu, Hoover, Warkentin, and Vandenberg (2008), who also found a major peak at T_{peak} ~ 72°C in pea flour, a system that contains more starch than protein. Peaks 2a, 2b, and 3, with the same transition temperatures as above, were obtained from the deconvolution of the merged peak (Figure 8, bottom). For the HPP treated mixed samples, only the merged peak was observed (Figure 8, top).

An analysis of the thermal transitions described above indicates that protein denaturation occurred after pressure treatment, as evidenced by the significantly lower protein denaturation enthalpy (Peak 3). This is consistent with prior observations (Sim et al., 2019).

For starch, the enthalpy of B-type starch gelatinization (Peak 2a) for both the untreated PPC and mixed samples (~2 J/g starch) was much smaller than for untreated pure pea starch (~32 J/g starch), which was attributed to the presence of lipids in the PPC powder. A decrease in the enthalpy of starch gelatinization in the presence of lipids was reported before (Eliasson, 1994). In contrast, the enthalpy of A-type starch gelatinization (Peak 2b) for the untreated PPC and mixed samples was similar to the untreated pure pea starch system. The peak temperatures of both B-type and A-type starch gelatinization for the untreated samples significantly increased with protein and starch content, which was likely due to reduced availability of water as more solids were added (Lund & Lorenz, 1984). Pure pea starch (8S sample) fully gelatinized under both heat and pressure treatments, as indicated by the lack of a gelatinization peak in Figure 7 (top panel). In contrast, starch in the PPC-only and mixed samples did not undergo pressure-gelatinization under the conditions used in this study. In fact, an increase in B-type starch gelatinization enthalpy (Peak 2a) was observed for all pressure-treated samples, although not all increases were statistically significant (Table 2). There were no significant changes in A-type starch gelatinization enthalpy with pressure treatment.

4 | DISCUSSION

Under the conditions used in this study, it appears that starch acted mainly as a filler in the pressure-induced pea protein gel matrix. The addition of starch enhanced the strength of the pressure-induced protein structures, and it enabled the formation of weak gels even at protein concentrations below the minimum required for gelation. This could be due to microscopic phase separation between starch and proteins (Colombo, León, & Ribotta, 2011), which reduced the volume occupied by protein molecules, leading to a localized increase in protein concentration. In the mixed pea protein–starch systems, the gel strength was however found to be more dependent on protein concentration, as the gel network was primarily made up by pressure denatured protein molecules.

Remarkably, starch granules in the pea protein–starch systems remained visually intact after pressure treatment. Thermal analyses further revealed that starch was not gelatinized in the pressure-treated samples. This could be due to the limited availability of water for starch gelatinization during the pressure treatment, since both protein and starch compete for water. In pressure treatment, protein denaturation occurs at a lower pressure than starch gelatinization. As water-holding capacity of the proteins increases after pressure denaturation (Queirós et al., 2018), this limits the amount of water available for starch gelatinization. It has been reported before that in the absence of water, pea starch did not gelatinize after HPP treatment (Leite et al., 2017). In contrast, heat-treated protein–starch systems of comparable total solids content to the present study led to the formation of starch and protein composite gels, with starch granules visibly disrupted by heat (Joshi et al., 2014; Li et al., 2007). Overall, this data demonstrates that the effect of high pressure on food components can be

very different than the effect of thermal treatments, particularly in complex systems.

5 | CONCLUSIONS

Low-temperature HPP treatment at 600 MPa for 4 min induced gel formation in mixed pea protein–starch systems, but starch remained ungelatinized and behaved as a filler in the protein gel matrix. This can have significant implications in the development of food products that contain pea protein, pea flour, or other plant-based ingredients using HPP technology. While ungelatinized starch contributes to structure formation, the presence of intact starch granules may impact the mouthfeel of the products, which needs to be tested using sensory evaluations. From a nutritional perspective, since ungelatinized starch is poorly digested and acts like a fiber (Wang & Copeland, 2013), pressure-treated protein–starch mixtures may allow the development of high protein products with a low glycemic index. The digestibility of HPP treated pea protein–starch mixtures is currently under investigation, and will shed further light on this issue.

ACKNOWLEDGMENTS

This work was funded by the USDA-NIFA grant 2016-67017-24635. The authors acknowledge the use of the DSC and electron microscope at the Cornell Center for Materials Research (CCMR), supported by NSF-MRSEC (DMR-1719875). The authors would like to thank Dr. Yifan Cheng from Cornell University for assistance with SEM imaging, AGT Foods for supplying the PPC powder, and World Food Processing for supplying the PS powder.

CONFLICT OF INTEREST

The authors declare no conflicts of interest.

ORCID

Carmen I. Moraru https://orcid.org/0000-0001-8307-7123

REFERENCES

Ahmed, J., Singh, A., Ramaswamy, H. S., Pandey, P. K., & Raghavan, G. S. V. (2014). Effect of high-pressure on calorimetric, rheological and dielectric properties of selected starch dispersions. *Carbohydrate Polymers*, *103*, 12–21. https://doi.org/10.1016/J.CARBPOL.2013.12.014

Ahmed, J., Varshney, S. K., & Ramaswamy, H. S. (2009). Effect of high pressure treatment on thermal and rheological properties of lentil flour slurry. *LWT—Food Science and Technology*, *42*(9), 1538–1544. https://doi.org/10.1016/J.LWT.2009.05.002

Angioloni, A., & Collar, C. (2013). Impact of high hydrostatic pressure on protein aggregation and rheological properties of legume batters. *Food and Bioprocess Technology*, *6*(12), 3576–3584. https://doi.org/10.1007/s11947-012-1020-5

Balasubramaniam, V. M., Martínez-Monteagudo, S. I., & Gupta, R. (2015). Principles and application of high pressure–based technologies in the food industry. *Annual Review of Food Science and Technology*, *6*(1), 435–462. https://doi.org/10.1146/annurev-food-022814-015539

Barrios-Peralta, P., Pérez-Won, M., Tabilo-Munizaga, G., & Briones-Labarca, V. (2012). Effect of high pressure on the interactions of myofibrillar proteins from abalone (Haliotis rufencens) containing several food additives. *LWT—Food Science and Technology*, *49*(1), 28–33. https://doi.org/10.1016/j.lwt.2012.04.025

Beliciu, C. M., & Moraru, C. I. (2013). Physico-chemical changes in heat treated micellar casein—soy protein mixtures. *LWT—Food Science and Technology*, *54*(2), 469–476. https://doi.org/10.1016/j.lwt.2013.06.013

Bogracheva, T. Y., Morris, V. J., Ring, S. G., & Hedley, C. L. (1998). The granular structure of C-type pea starch and its role in gelatinization. *Biopolymers*, *45*(4), 323–332 https://doi.org/10.1002/(SICI)1097-0282(19980405)45:4<323::AID-BIP6>3.0.CO;2-N

Buerman, E. C., Worobo, R. W., & Padilla-Zakour, O. I. (2020). High pressure processing of spoilage fungi as affected by water activity in a diluted apple juice concentrate. *Food Control*, *107*, 106779. https://doi.org/10.1016/j.foodcont.2019.106779

Cadesky, L., Walkling-Ribeiro, M., Kriner, K. T., Karwe, M. V., & Moraru, C. I. (2017). Structural changes induced by high-pressure processing in micellar casein and milk protein concentrates. *Journal of Dairy Science*, *100*(9), 7055–7070. https://doi.org/10.3168/jds.2016-12072

Chung, H.-J., Liu, Q., Hoover, R., Warkentin, T. D., & Vandenberg, B. (2008). In vitro starch digestibility, expected glycemic index, and thermal and pasting properties of flours from pea, lentil and chickpea cultivars. *Food Chemistry*, *111*(2), 316–321. https://doi.org/10.1016/J.FOODCHEM.2008.03.062

Colombo, A., León, A. E., & Ribotta, P. D. (2011). Rheological and calorimetric properties of corn-, wheat-, and cassava- starches and soybean protein concentrate composites. *Starch/Staerke*, *63*(2), 83–95. https://doi.org/10.1002/star.201000095

Eliasson, A. C. (1994). Interactions between starch and lipids studied by DSC. *Thermochimica Acta*, *246*(2), 343–356. https://doi.org/10.1016/0040-6031(94)80101-0

Grauwet, T., Van der Plancken, I., Vervoort, L., Hendrickx, M., & Van Loey, A. (2016). High-pressure processing uniformity. In *Food Engineering Series* (pp. 268–253). New York, NY: Springer. https://doi.org/10.1007/978-1-4939-3234-4_13

Henchion, M., Hayes, M., Mullen, A., Fenelon, M., & Tiwari, B. (2017). Future protein supply and demand: Strategies and factors influencing a sustainable equilibrium. *Food*, *6*(7), 53. https://doi.org/10.3390/foods6070053

Hunt, A., Getty, K. J. K., & Park, J. W. (2009). Roles of starch in surimi seafood: A review. *Food Reviews International*, *25*(4), 299–312. https://doi.org/10.1080/87559120903155834

Joshi, M., Aldred, P., Panozzo, J. F., Kasapis, S., & Adhikari, B. (2014). Rheological and microstructural characteristics of lentil starch-lentil protein composite pastes and gels. *Food Hydrocolloids*, *35*, 226–237. https://doi.org/10.1016/j.foodhyd.2013.05.016

Leite, T. S., de Jesus, A. L. T., Schmiele, M., Tribst, A. A. L., & Cristianini, M. (2017). High pressure processing (HPP) of pea starch: Effect on the gelatinization properties. *LWT—Food Science and Technology*, *76*, 361–369. https://doi.org/10.1016/j.lwt.2016.07.036

Li, J. Y., Yeh, A. I., & Fan, K. L. (2007). Gelation characteristics and morphology of corn starch/soy protein concentrate composites during heating. *Journal of Food Engineering*, *78*(4), 1240–1247. https://doi.org/10.1016/j.jfoodeng.2005.12.043

Lund, D., & Lorenz, K. J. (1984). Influence of time, temperature, moisture, ingredients, and processing conditions on starch gelatinization. *Critical Reviews in Food Science and Nutrition*, *20*(4), 249–273. https://doi.org/10.1080/10408398409527391

Murtey, M. D., & Ramasamy, P. (2016). Sample preparations for scanning electron microscopy – Life sciences. In *Modern Electron Microscopy in Physical and Life Sciences*. Retrieved from https://www.intechopen.com/books/modern-electron-microscopy-in-physical-and-life-sciences/sample-preparations-for-scanning-electron-microscopy-life-sciences.

Oh, H. E., Anema, S. G., Pinder, D. N., & Wong, M. (2009). Effects of different components in skim milk on high-pressure-induced gelatinisation

of waxy rice starch and normal rice starch. *Food Chemistry*, *113*(1), 1–8. https://doi.org/10.1016/j.foodchem.2008.07.107

Pei-Ling, L., Xiao-Song, H., & Qun, S. (2010). Effect of high hydrostatic pressure on starches: A review. *Starch—Stärke*, *62*(12), 615–628. https://doi.org/10.1002/star.201000001

Queirós, R. P., Saraiva, J. A., & da Silva, J. A. L. (2018). Tailoring structure and technological properties of plant proteins using high hydrostatic pressure. *Critical Reviews in Food Science and Nutrition*, *58*(9), 1538–1556. https://doi.org/10.1080/10408398.2016.1271770

Ratnayake, W. S., Hoover, R., Shahidi, F., Perera, C., & Jane, J. (2001). Composition, molecular structure, and physicochemical properties of starches from four field pea (*Pisum sativum* L.) cultivars. *Food Chemistry*, *74*(2), 189–202. https://doi.org/10.1016/S0308-8146(01)00124-8

Shand, P. J., Ya, H., Pietrasik, Z., & Wanasundara, P. K. J. P. D. (2007). Physicochemical and textural properties of heat-induced pea protein isolate gels. *Food Chemistry*, *102*(4), 1119–1130. https://doi.org/10.1016/j.foodchem.2006.06.060

Sim, S. Y. J., Karwe, M. V., & Moraru, C. I. (2019). High pressure structuring of pea protein concentrates. *Journal of Food Process Engineering*, *42*(7), e13261. https://doi.org/10.1111/jfpe.13261

Steffe, J. F. (1996). *Rheological methods in food process engineering*. East Lansing, MI: Freeman Press.

Wang, S., & Copeland, L. (2013). Molecular disassembly of starch granules during gelatinization and its effect on starch digestibility: A review. *Food and Function*, *4*(11), 1564–1580. https://doi.org/10.1039/c3fo60258c

Yang, Z., Chaib, S., Gu, Q., & Hemar, Y. (2017). Impact of pressure on physicochemical properties of starch dispersions. *Food Hydrocolloids*, *68*, 164–177. https://doi.org/10.1016/j.foodhyd.2016.08.032

Zhang, Y., Liu, X. C., Wang, Y., Zhao, F., Sun, Z., & Liao, X. (2016). Quality comparison of carrot juices processed by high-pressure processing and high-temperature short-time processing. *Innovative Food Science and Emerging Technologies*, *33*, 135–144. https://doi.org/10.1016/j.ifset.2015.10.012

SUPPORTING INFORMATION

Additional supporting information may be found online in the Supporting Information section at the end of this article.

How to cite this article: Sim SYJ, Moraru CI. High-pressure processing of pea protein–starch mixed systems: Effect of starch on structure formation. *J Food Process Eng*. 2019; e13352. https://doi.org/10.1111/jfpe.13352